

Can faults become barriers for deep fluid circulation? Insights from high-resolution seismic VSP tomography at the Soultz-sous-Forêts geothermal site

Marco Calò, Catherine Dorbath, Paul Lubrano Lavadera

▶ **To cite this version:**

Marco Calò, Catherine Dorbath, Paul Lubrano Lavadera. Can faults become barriers for deep fluid circulation? Insights from high-resolution seismic VSP tomography at the Soultz-sous-Forêts geothermal site. Geophysical Research Letters, 2016, 43, pp.8986-8993. 10.1002/2016GL069623 . insu-03707897

HAL Id: insu-03707897

https://insu.hal.science/insu-03707897

Submitted on 29 Jun 2022

HAL is a multi-disciplinary open access archive for the deposit and dissemination of scientific research documents, whether they are published or not. The documents may come from teaching and research institutions in France or abroad, or from public or private research centers.

L'archive ouverte pluridisciplinaire **HAL**, est destinée au dépôt et à la diffusion de documents scientifiques de niveau recherche, publiés ou non, émanant des établissements d'enseignement et de recherche français ou étrangers, des laboratoires publics ou privés.

Copyright

AGU PUBLICATIONS

Geophysical Research Letters

RESEARCH LETTER
10.1002/2016GL069623

Key Points:
- High-resolution VSP tomography images a thin structure in geothermal system
- Faults can affect deep fluid circulation between geothermal wells
- Orientation of the faults can drive massive injections of fluids

Supporting Information:
- Supporting Information S1

Correspondence to:
M. Calò,
calo@geofisica.unam.mx;
marcoocalo@yahoo.it

Citation:
Calò, M., C. Dorbath, and P. Lubrano Lavadera (2016), Can faults become barriers for deep fluid circulation? Insights from high-resolution seismic VSP tomography at the Soultz-sous-Forêts geothermal site, *Geophys. Res. Lett.*, *43*, 8986–8993, doi:10.1002/2016GL069623.

Received 16 MAY 2016
Accepted 13 JUL 2016
Accepted article online 15 JUL 2016
Published online 14 SEP 2016

©2016. American Geophysical Union. All Rights Reserved.

Can faults become barriers for deep fluid circulation? Insights from high-resolution seismic VSP tomography at the Soultz-sous-Forêts geothermal site

Marco Calò[1], Catherine Dorbath[2], and Paul Lubrano Lavadera[3]

[1]Instituto de Geofísica, Universidad Nacional Autonoma de Mexico, Mexico City, Mexico, [2]Ecole et Observatoire des Sciences de la Terre, University of Strasbourg, Strasbourg, France, [3]NORSAR, Oslo, Norway

Abstract Vertical Seismic Profile (VSP) surveys are generally used for modelling converted phases of the seismic body waves propagating in the medium allowing the detection of waves interpreted as reflections on steeply dipping reflecting structures such as faults, abrupt lateral changes of lithology, and fractures. At the Enhanced Geothermal System geothermal field of Soultz-sous-Forêts the analysis of data recorded during a VSP experiment allowed describing the presence of at least two structures near the wells. Here we show how seismic tomography method can be applied to the VSP data to reconstruct the 3-D shape of structures in the volume surrounding the geothermal wells. The three-dimensional *P* wave velocity model obtained shows positive velocity anomalies associated with the main faults observed by the VSP analysis and negative anomalies in the regions affected by massive hydraulic stimulations performed in the past. This pattern can be explained as a different response of the rock volume to the fluid injections where regions marked by relative pre-existing high permeability were less affected by the hydraulic stimulations. This difference in permeability produced regions that could work as barriers for fluid diffusion through the reservoir. Comparisons of our high resolved model with the location of the induced seismicity and with another model obtained using seismic noise correlation give evidence of the presence of these structures and may explain the poor connection between the wells GPK4 and GPK2–GPK3 system.

1. Introduction

The performance of an Enhanced Geothermal System (EGS) is related to the hydraulic connectivity of the injection and production boreholes. Injection tests can play an important role for increasing the general permeability of the reservoir around the wells. However, sometimes, the results of the stimulations are not satisfactory in the sense that the increased permeability and connections between boreholes are lower than expected. These drawbacks limit the productivity of the geothermal reservoir resulting in a big impact of its economical sustainability.

In Alsace, at the EGS geothermal field of Soultz-sous-Forêts three wells (GPK2, GPK3, GPK4) reach a depth of about 5000 m (Figure 1). Each well is distant from the other approximately 600 m at the depth of the reservoir exploitation (occurring between 4000 m and 5000 m). In order to connect the boreholes to the fracture network efficiently and to improve the global permeability of the reservoir, GPK2 was stimulated in June/July 2000, GPK3 in May/June 2003, and GPK4 in September 2004 and again in February 2005. An acidified water injection experiment was also conducted in GPK4 in February/March 2005. Presently, the reservoir development is completed and exploitation of heat is conducted through a geothermal reservoir whose depth ranges from 4000 to 5000 m. During the stimulation of the three wells, several thousand induced seismic events were detected and located and used for describing the seismic response of the reservoir [*Charléty et al.*, 2007; *Cuenot et al.*, 2008; *Dorbath et al.*, 2009; *Calò et al.*, 2011; *Calò and Dorbath*, 2013; *Calò et al.*, 2014].

After the stimulations, tracer tests were conducted using organic compounds giving evidence of different types of hydraulic paths between the wells that are resumed in four loops [*Sanjuan et al.*, 2006]: (i) a fast and relatively direct hydraulic connection between GPK2 and GPK3 (short loop), (ii) the existence of a larger and slower hydraulic connection between GPK2 and GPK3 (large loop), (iii) a poor connection between GPK3 and GPK4, and (iv) a much large-scale loop connecting GPK4 to GPK2 and GPK3 rather than to a direct connection to GPK3. Therefore, the results of the tracer tests highlighted the presence of a sort of "barrier" separating hydraulically the well GPK4 and the GPK2-GPK3 system.

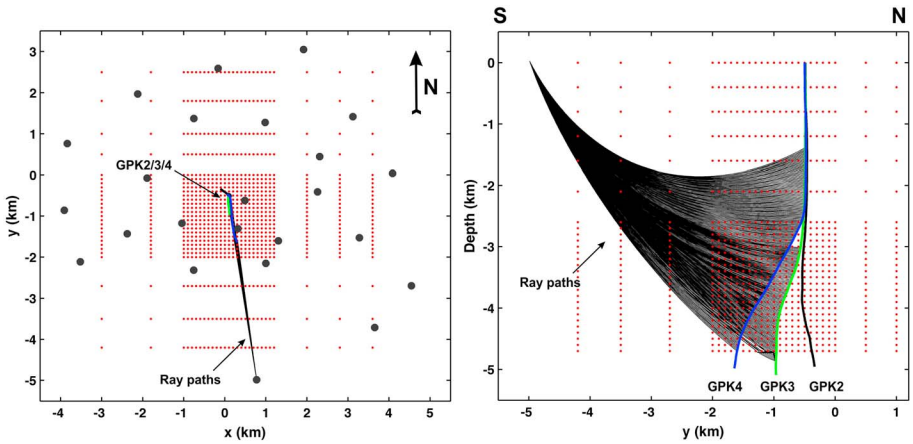


Figure 1. (left) Map of the sources (black dots) used for the VSP survey and to perform the seismic tomography. Red dots are the positions of the grid nodes used for the tomographic inversion. Projections of the wells GPK2/3/4 and of the seismic ray paths of one source are also reported. (right) Vertical projection of the seismic ray paths between one source and the geophones located into the wells GPK3 and GPK4. Note the density of the ray paths. Red dots are the nodes of the inversion grid.

Kohl et al. [2006] studying the event density distribution suggested the presence of a conductive structure between GPK3 and GPK4 that contrasted the migration of the seismicity during the injection of GPK4 and partially that of GPK3.

Nevertheless, both tracer tests and studies based on the spatial density of the seismicity do not give a direct proof of the existence of a structure for the simply reason that (i) tracer test gives insight on the connectivity between wells and apparent permeability of the reservoir and it is not able to depicts shape, direction, dip of permeable structures and (ii) standard location procedure of seismicity at Soultz produces horizontal and vertical uncertainty of 100 m and 80 m [*Cuenot et al.*, 2008]. These errors on the event locations may introduce large bias on the evaluation of the direction and dip of thin structures (e.g., less than 300–200 m thick). Therefore, the use of the Soultz catalogues needs more processing to refine the event location for studying thin structures [e.g., *Calò et al.*, 2011; *Calò and Dorbath*, 2013].

Place et al. [2011] used the data acquired during a first VSP survey performed in 1993 to describe the main fault geometry in the first 3500 m of the reservoir and extrapolating it to the deeper part. *Sausse et al.* [2010] combined all the existing information from well logs, induced seismicity, and active sources showing a complex network of structures affecting the reservoir.

However, the presence of such hydraulic barrier and its nature is still under debate because of the lack of geophysical/geological information at depths greater than 3500 m.

In 2007 a Vertical Seismic Profile (VSP) multicomponent, multioffset survey has been conducted in the wells GPK3 and GPK4 down to 4800 m depth. The records have been used for modelling converted phases of the body waves propagating in the granite allowing the detection of waves interpreted as reflections on steeply dipping reflectors intersecting the wells between 4 and 5 km depth [*Lubrano Lavadera,* 2013]. The main results of that study were (a) a better constrain of the direction of the major NW-SE fault crossing the wells and (b) the observation of a reflecting structure located westward of the reservoir between GPK3 and GPK4 and striking NE-SW, which was not observed with the previous active seismic surveys.

In this work we performed a 3-D high-resolution seismic tomography using the first arrival times picked on the records of the VSP survey. Since sources and sensors have known position, the errors produced on the seismic velocity estimations are strongly reduced, allowing a more reliable interpretation also of the weak anomalies. Here we show that the reconstructed seismic velocity model depicts patterns highly correlated with the geometry of the faults described with the classical VSP analysis by *Lubrano Lavadera* [2013]. Comparison of the VSP results presented here, with those of an independent experiment carried out using the seismic noise cross-correlation (NCC) tomography [*Calò et al.*, 2013a], and with the spatial distribution of the induced seismicity corroborates the pattern observed. The velocity model presented here,

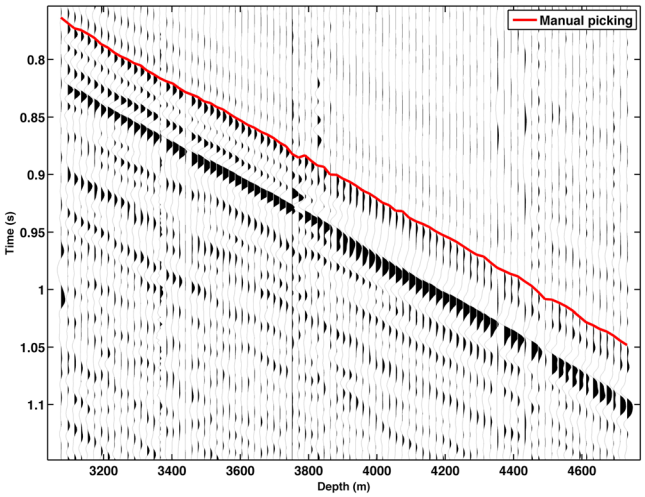


Figure 2. Example of signals recorded at the geophones located in the well GPK3. Red line refers to the manual picking of the first arrivals.

complemented with the VSP analysis, allows describing the presence of structures that play a crucial role on the fluid circulation and that can justify the poor connection between the wells GPK3 and GPK4. Some of these structures are not necessarily seismically active because they are highly permeable and unfavorably oriented with respect to the main direction of the regional stress acting in the study area.

2. Data and Method

We used data collected during a VSP survey performed in 2007. The experiment was conducted locating two arrays of three component geophones in the wells GPK3 and GPK4 at a depth range of 2.84–4.81 km and 3.09–4.81 km, respectively. The spacing of the geophones was 20 m, and the signals were recorded with a sampling rate of 500 Hz. The sources consisted of 24 shot points located within a 5 km radius around the well head and recorded by two sets of geophones located into the two wells (Figure 1). We picked the first arrival time of each trace manually by keeping only the signals marked by a high signal-to-noise ratio for a total of 2880 *P* wave travel time measurements. Figure 2 reports an example of the signals recorded during a shot and the picking of the first arrival times. The errors associated with the picking procedure can be estimated on 0.002 s.

The database was then used for calculating a *Vp* model applying the travel time local earthquake tomography method [*Evans et al.,* 1994]. The initial horizontal nodes spacing for the seismic velocity inversion is 75 m in the *X*, *Y*, and *Z* directions near the centre of the grid, where a maximal resolution is required, whereas it is sparser in the rest of the investigated volume (Figure 1).

The initial 1-D horizontally layered velocity model used is derived from sonic logs and calibration shots performed in the GPK1 well [*Beauce et al.,* 1991]. This model is the same used to locate the induced seismicity observed during injections tests and for the seismic monitoring. To be consistent with the previous studies related to the induced seismicity [*Charléty et al.*, 2007; *Cuenot et al.*, 2008; *Dorbath et al.*, 2009; *Calò et al.*, 2011; *Calò and Dorbath*, 2013; *Calò et al.*, 2014], we chose GPK1 well head (48.93537 N, 7.86535 E, altitude 153 m) as the geographical origin for the grid points.

We imposed only velocity adjustments during the inversion procedure because source position and origin time are known. The computation of the final velocity model has been obtained applying the weighted average model (WAM) postprocessing [*Calò*, 2009; *Calò et al.*, 2009, 2011, 2013b]. In WAM, several velocity models are calculated using different input parameters and merged into a final velocity distribution. This technique allows to significantly reduce the input parameter effects on the final velocity distribution making the model more reliable [*Calò et al.*, 2011; *Calò et al.*, 2012]. Hence, we merged seven velocity models obtained after perturbing the position of the velocity nodes by rotating the inversion grid by 30° steps and changing the position of the nodes in depth. The relative small amount of models merged with WAM is due to the fact that for this experiment, the parameter most affecting the results was the inversion grid (origin time of and position of the sources are known). We assessed the reliability of the features observed on the *P* wave velocity model performing a restoration resolution (RR) test [*Zhao et al.*, 1992]. RR test (Figure S1 in the supporting information) shows that at depth of 4 km, seismic structures 200 m thin are sufficiently recovered in a region of about 1×1 km^2 centred on the wells. In vertical direction, the model is well recovered in the depth range of 3.5–4.7 km. However, the lateral extension of the best resolved region decreases with depth, making difficult at 4.5–4.7 km the interpretation of the structure at distance grater 200 m from the wells GPK3/4. Analysis of the resolution matrix (Figure S2) shows that the inversion procedure is well constrained by the data in the study region. Although at depths shallower than 4 km, the model is still resolved at distance greater than

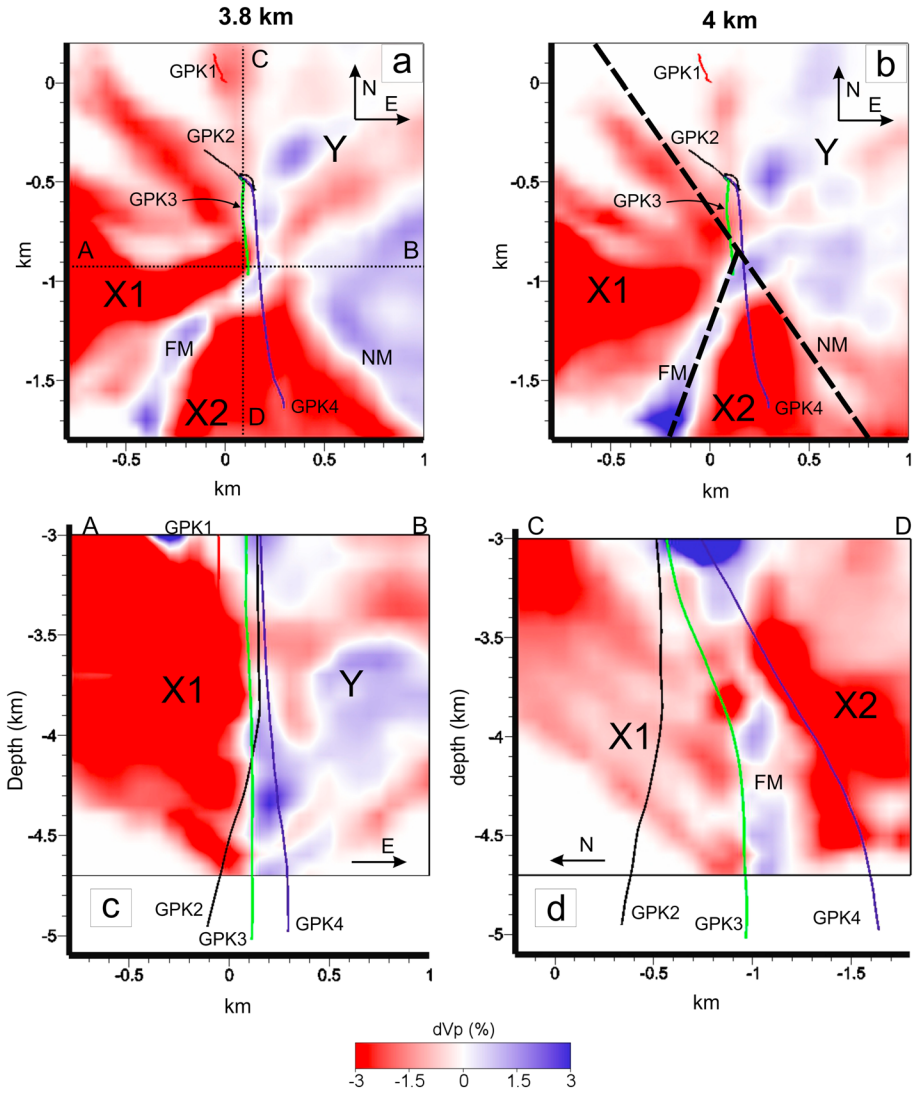


Figure 3. (top) Maps of the *P* wave anomalies at (a) 3.8 km and (b) 4 km depth. In each map is also projected; the positions of the wells (GPK1/2/3/4), the direction of the reflecting faults modelled by the VSP analysis, and the traces of the cross sections (A-B and C-D). (bottom) Vertical sections of the *P* wave anomaly along the profile A-B and C-D. The projection of the wells is also reported.

500–1000 m from the wells, smearing affects due to the poor intersection of the ray paths make the interpretation not reliable; therefore, all our considerations refer to the volume around the injection wells.

3. Results and Discussion

The *P* wave velocity model reported here is expressed in percentage with respect to the initial 1-D model. The horizontal slices at 3.8 km and 4.0 km depth (Figures 3a and 3b) show that the investigated volume is split into two main domains: a region marked by a positive anomaly located east of the wells (up to 3%, marked with Y in Figure 3) and a region mostly dominated by a negative one in the west sector (X1 and X2, in Figures 3a and 3b). The separation region (NM, dashed line in Figure 3b) is oriented approximately NNW-SSE. Furthermore, a thin (less than 200 m) high *Vp* anomaly (FM, dashed line in Figure 3b) oriented SW-NE is located between the wells GPK3 and GPK4 splitting the low-velocity anomaly in two subregions (X1 and X2). Vertical section A-B (Figure 3c) shows the continuity of the pattern observed for the structure NM, at least in the depth range of 3.5–4.7 km (i.e., in the well resolved part of the model), whereas section C-D shows the continuity of FM in depth.

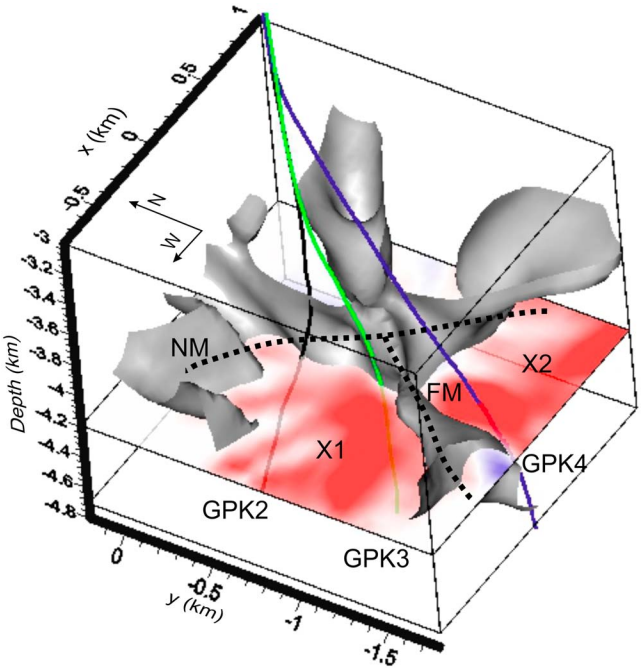


Figure 4. A 3-D plot of the high *Vp* anomalies (larger than 1%). Dashed lines (NM and FM) are the main faults discussed in the text. A slice shows the X1 and X2 low-velocity regions at 4.2 km depth. The trajectory of the wells GPK2, GPK3, and GPK4 is also reported.

In our model, we interpret the low *Vp* anomalies (X1 and X2) as an expression of the volume affected by the previous hydraulic stimulations performed to increase the reservoir performance. On the other hand we interpret the positive velocity anomaly FM as expression of a region marked by a relative high permeability before the injection periods that has been affected only marginally by the injections tests. Finally, we associate the structure NM with a main fault, which controls the large-scale fluid circulation and separating the reservoir in two sectors; one more permeable because damaged by the injections tests (X1 and X2) and another one (Y) less damaged because injected fluids did not propagate beyond NM.

Lubrano Lavadera [2013], using the same database for the VSP analysis described the presence of at least two main reflecting structures near the wells GPK3 and GPK4 (dashed lines in Figure 3b). The first one is compatible with the fault plane region oriented NNW-SSE and already observed by several authors because crossing the well GPK3 at about 4.76 km depth [*Sausse et al.*, 2010; *Dorbath et al.*, 2009]. The second structure, although other authors have proposed its presence, is illuminated for the first time thanks to the survey of 2007 [*Lubrano Lavadera*, 2013]. The projection of the two faults on the horizontal section of the *Vp* model shows the good agreement existing between the orientations of the structures observed with the VSP modelling and the seismic velocity pattern presented here (Figure 3b).

Therefore, we suppose that the injection tests performed at Soultz allowed the reactivation of the fracture network producing a huge amount of induced seismicity due to the pore pressure increase and consequently an increase of permeability. The relative lowering of Vp is due to the damaging of the rock volume [*Shalev et al.*, 2013] and change of the original stress condition. Therefore, injection tests can cause lowering of the seismic velocities and increasing of permeability. Laboratory experiments also show the trend where an increase of permeability produces a lowering of the seismic velocities [*Barton*, 2006; *Klimentos*, 1991]. In regions where the permeability is already high, the lowering of the *Vp* is less noticeable. This has already been observed during the stimulation of GPK3 in 2003 where the decrease of the seismic *P* wave velocities were of only 1–3% with respect to the reference value because most of the injection water was absorbed by an open fracture crossing the borehole [*Calò and Dorbath*, 2013].

Therefore, the goal of the injections test (i.e., to increase the permeability of a reservoir) is strongly affected by the presence of large pre-existing high-permeability structures [*Calò and Dorbath*, 2013; *Dorbath et al.*, 2009; *Nami et al.*, 2008]. If a large fracture crosses the well, most of the injected water is drained through, and weak overpressures in the volume are expected. In this condition, if induced events occur, the fault plane region plays an important role on driving the seismicity [*Calò and Dorbath*, 2013; *Wibberley and Shimamoto*, 2003; *Byerlee*, 1990]. If the permeable/fault zone is relatively close to the injection point, the stimulation allows an increasing of the pore pressure only in the volume between the borehole and the structure. Indeed the relatively larger pre-existing permeability affects the pore pressure changes beyond the structure and consequently the microseismic occurrence. Consequently, in some circumstances a structure marked by a larger permeability than the surrounding region, such as an open fault, can be considered as a barrier

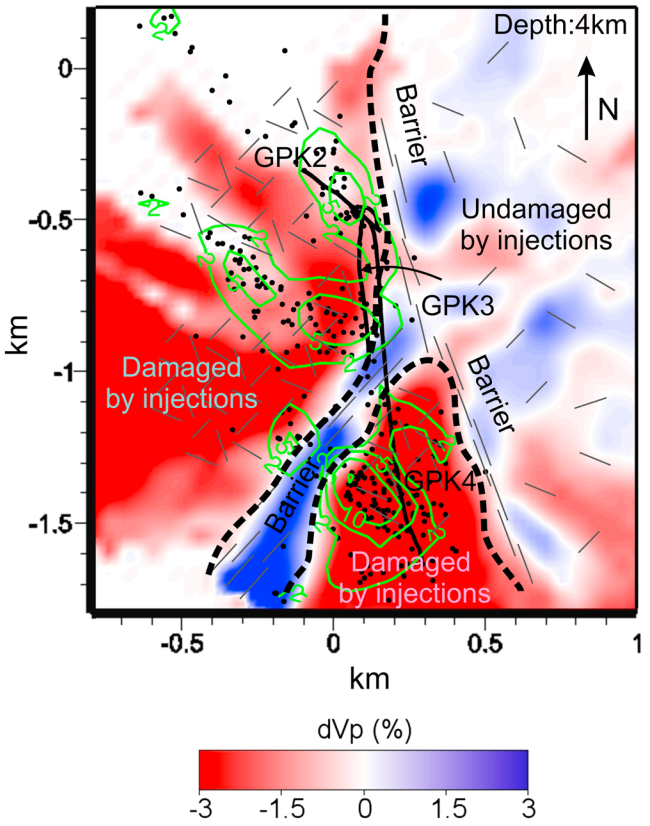


Figure 5. Sketch showing how the low *Vp* anomalies are the regions damaged by the injections and high *Vp* anomalies are expression of structures undertaking the role of barriers for fluid circulation between the wells. The black dots are the projections of the events with duration magnitude greater than 0.3 recorded during the injection tests of 2000, 2003, 2004, and 2005 and located ±200 m from the depth of the corresponding slice. The events are located using both 3-D models and double difference data (for details see *Calò et al.* [2011], *Calò and Dorbath* [2013], and *Calò et al.* [2014]). Green lines contour the density event in pixels of 150 × 150 m. Numbers on the green lines indicate the event density of the pixels.

that avoids (i) the propagation of the fluids beyond the fault (ii) consequently the variation of pore pressure, (iii) the possible occurrence of induced seismicity, (iv) and the consequent increase of permeability beyond the structure.

NM has likely influenced all the injection tests performed in the area avoiding the fracturation/optimization of the reservoir in the east side. This hypothesis of fault-driven stimulation is given by the fact that the seismicity of all the injections and circulations tests performed at Soultz occurred mostly in the western (and northern) side of the EGS. The high contrasts in velocity observed between the eastern side and western one on our *Vp* model support the idea that NM represents a fault bordering the easternmost side of the EGS. Furthermore, a recent *Vs* model of the region, obtained applying the noise cross-correlation tomography technique [*Calò et al.*, 2013a], reports exactly the same pattern, i.e., a low-velocity anomaly located only eastward to the wells (Figure S3). The region separating the high and low anomalies matches for both models suggesting that the structure NM plays a role on the velocity pattern both for *Vp* and *Vs*.

The presence of FM, although not observed on the NCC model because of the lack of resolution, is documented by the VSP analysis suggesting the existence of a relatively thin region containing reflecting fault planes [*Lubrano Lavadera*, 2013].

Projections of the best located events related to all the injections tests on the velocity model (Figure S3) show that the events are mostly located in the low-velocity regions highlighting that the stimulations of the wells GPK2 and GPK3 affected mostly the region north of FM, whereas those of GPK4 developed the reservoir south of it. The presence of FM has affected indirectly the seismic pattern of the induced seismicity observed during the GPK4 stimulations [*Calò et al.*, 2014]. The seismic clouds observed during those injections did not propagate northward and had a shape of segment of ring vertically oriented with a seismic gap in the region where FM has been observed (Figure S4).

A three-dimensional plot of the high-velocity anomaly (Figure 4) shows that NM fault limits the eastern side of the reservoir from the western one, while FM splits, at all depths (3.8–4.6 km depth), the western sector into a northern part, where it operates the wells GPK2 and GPK3, from the southern one, which includes the region of interest of the well GPK4.

All these considerations are based on the assumption that all the parts in which the reservoir is nowadays separated (X1, X2, and Y) had similar physical characteristics before the stimulations, and what we are observing now is a consequence of the massive injections performed at Soultz.

The sketch of Figure 5 schematizes the pattern observed and its interpretation. Overlapped to the model are the projections of the best located events ($Md > 0.3$) induced during the injection tests performed between 2000 and 2005, highlighting that the low *Vp* zones are the most affected by the seismicity. Following these observations, we argue that the two structures constrain the fluid circulation reducing strongly the connectivity between GPK4 and the other wells as was already documented by the tracer tests performed to assess the injection performance [*Sanjuan et al.*, 2006]. In addition, spatial coherence between seismicity and low *Vp* anomalies supports the idea that these lasts are portions of the reservoir involved by the injections, which are separated in subregions because of the fault zones.

4. Conclusion

In this work we showed a high resolved 3-D *P* wave velocity model obtained using *P* wave travel times picked on the signals recorded during the VSP experiment performed in 2007 at the geothermal reservoir of Soultz-sous-Forêts.

The seismic pattern observed here is in agreement with the structures imaged with the classical analysis of these data (i.e., the reconstruction of structures by analysis of the reflected/converted phases). The main fault crossing the reservoir is identified as a clear limit between higher and lower *Vp* zones. Furthermore, this pattern has been documented by an independent experiment using the seismic noise cross-correlation tomography [*Calò et al.*, 2013a].

We also showed the evidence of a structure, which was already suggested by other authors [e.g., *Kohl et al.*, 2006; *Sausse et al.*, 2010] but never clearly documented. This structure is underlined by both reflections through classical VSP analysis and the *Vp* model proposed here, which images a thin (less than 200 m) high-velocity anomaly. This structure is located between the wells GPK3 and GPK4, affected the injections tests of GPK4 in 2004/5 and the related induced seismicity [*Calò et al.*, 2014], and could represent a valid element to explain the low connection between the southern and northern parts of the reservoir.

Finally, here we showed that VSP data can be used not only for describing possible dipping reflectors but also for seismic velocity models, which complements the information retrieved by the classical use of such data.

Acknowledgments
Data of VSP are available at the EOST, University of Strasbourg, and at the GEIE, Exploitation Minière de la Chaleur. During this work M. Calò was funded by the GEISER European Project (FP7: 241321). We thank Philippe Jousset and the two anonymous reviewers for their comments, which improved this manuscript.

References

Barton, N. (2006), *Rock Quality, Seismic Velocity, Attenuation and Anisotropy*, pp. 1–756, CRC Press.
Beauce, A., H. Fabriol, D. Le Masne, C. Cavoit, C. Mechler, and X. Chen (1991), Seismic studies on the HDR site of Soultz-sous-Forêts (Alsace, France), *Geotherm. Sci. Tech.*, *4*, 239–266.
Byerlee, J. (1990), Friction, overpressure and fault normal compression, *Geophys. Res. Lett.*, *17*, 2109–2112, doi:10.1029/GL017i012p02109.
Calò, M. (2009), Tomography of subduction zones using regional earthquakes: methodological developments and application to the Ionian slab, PhD Thesis. [Available at http://tel.archives-ouvertes.fr/tel-00438598/en/.]
Calò, M., and C. Dorbath (2013), Different behaviours of the seismic velocity field at Soultz-sous-Forêts revealed by 4D seismic tomography: case study of GPK3 and GPK2 injection tests, *Geophys. J. Int.*, *194*(3), 1893–1899, doi:10.1093/gji/ggt153.
Calò, M., C. Dorbath, D. Luzio, S. R. Rotolo, and G. D'Anna (2009), Local Earthquakes Tomography in the southern Tyrrhenian region: Geophysical and petrological inferences on subducting lithosphere, in *Subduction Zone Dynamics Series: Frontiers in Earth Sciences*, edited by S. Lallemand and F. Funiciello, vol. XX, p. 276, doi:10.1007/978-3-540-87974-9.
Calò, M., C. Dorbath, F. H. Cornet, and N. Cuenot (2011), Large-scale aseismic motion identified through 4-D P-wave tomography, *Geophys. J. Int.*, *186*, 1295–1314, doi:10.1111/j.1365-246X.2011.05108.x.
Calò, M., C. Dorbath, D. Luzio, S. G. Rotolo, and G. D'Anna (2012), Seismic velocity structures of southern Italy from tomographic imaging of the Ionian slab and petrological inferences, *Geophys. J. Int.*, *191*, 751–764, doi:10.1111/j.1365-246X.2012.05647.x.
Calò, M., X. Kinnerat, and C. Dorbath (2013a), Procedure to construct three-dimensional models of geothermal areas using seismic noise cross-correlations: Application to the Soultz-sous-Forêts enhanced geothermal site, *Geophys. J. Int.*, *194*(3), 1893–1899, doi:10.1093/gji/ggt205.
Calò, M., L. Parisi, and D. Luzio (2013b), Lithospheric *P* and *S* wave velocity models of the Sicilian area using WAM tomography: procedure and assessments, *Geophys. J. Int.*, *195*(1), 625–649, doi:10.1093/gji/ggt252.
Calò, M., C. Dorbath, and M. Frogneux (2014), Injection tests at the EGS reservoir of Soultz-sous-Forêt. Seismic response of the GPK4 stimulations, *Geothermics*, *52*, 50–58, doi:10.1016/j.geothermics.2013.10.007.
Charléty, J., N. Cuenot, L. Dorbath, C. Dorbath, H. Haessler, and M. Frogneux (2007), Large earthquakes during hydraulic stimulations at the geothermal site of Soultz-sous-Forêts, *Int. J. Rock Mech. Min. Sci.*, *44*, 1091–1105.
Cornet, F. H., T. Berard, and S. Bourouis (2007), How close to failure is a natural granite rock mass at 5 km depth, *Int. J. Rock Mech. Min. Sci.*, *44*(1), 47–66.
Cuenot, N., C. Dorbath, and L. Dorbath (2008), Analysis of the microseismicity induced by fluid injections at the EGS Site of Soultz-sous-Forêts (Alsace, France): Implications for the characterization of the geothermal reservoir properties, *Pure Appl. Geophys.*, *165*, 797–828.
Dorbath, L., N. Cuenot, A. Genter, and M. Frogneux (2009), Seismic response of the fractured and faulted granite of Soultz-sous-Forêts (France) to 5 km deep massive water injections, *Geophys. J. Int.*, *177*, 653–675.
Evans J. R., D. Eberhart-Phillips, and C. H. Thurber (1994), User's manual for SIMULPS12 for imaging vp and vp/vs; a derivative of the "Thurber" tomographic inversion SIMUL3 for local earthquakes and explosions. [Available at pubs.er.usgs.gov.]
Klimentos, T. (1991), The effects of porosity-permeability-clay content on the velocity of compressional waves, *Geophysics*, *56*, 1930–1939.

Kohl, T., C. Baujard, and T. Mégel (2006), Conditions for mechanical re-stimulation of GPK4, Conference paper presented at EHDRA Scientific Conference, 15–16 June 2006, Soultz-sous-Forêts, France.

Lubrano Lavadera, P. (2013), Traitement des données de sismique de puits acquises en 2007 sur le site de Soultz-sous-Forêts pour la caractérisation de la fracturation du réservoir géothermique, Université de Strasbourg, French, NNT: 2013STRAH013, Tel-01038001.

Nami, P., R. Schellschmidt, M. Schindler, and T. Tischner (2008), Chemical stimulation operations for reservoir development of the deep crystalline HDR/EGSsystem at Soultz-sous-Forêts (France), Proceedings, 33rd Workshop on Geothermal Reservoir Engineering, Stanford University, Stanford, CA, January 28–30.

Place, J., J. Sausse, D. Diraison, Y. Géraud, C. Naville, and J. M. Marthelot (2011), 3D mapping of permeable structures affecting a deep granite basement from isotropic 3C VSP data, *Geophys. J. Int.*, *186*, 245–263.

Sanjuan, B., J. L. Pinault, P. Rose, A. Gérard, M. Brach, G. Braibant, C. Crouzet, J. C. Foucher, A. Gautier, and S. Touzelet (2006), Tracer testing of the geothermal heat exchanger at Soultz-sous-Forêts (France) between 2000 and 2005, *Geothermics*, *35*(Special Issue), 622–653.

Sausse, J., C. Dezayes, L. Dorbath, A. Genter, and J. Place (2010), 3D fracture zone network at Soultz based on geological data, image logs, microseismic events and VSP results, *C. R. Geosci.*, *342*, 531–545.

Shalev, E., M. Calò, and V. Lyakhovsky (2013), Formation of damage zone and seismic velocity variations during hydraulic stimulation: Numerical modeling and field observations, *Geophys. J. Int.*, *195*(2), 1023–1033, doi:10.1093/gji/ggt279.

Wibberley, C. A. J., and T. Shimamoto (2003), Internal structure and permeability of major strike-slip fault zones: The Median Tectonic Line in Mie Prefecture, Southwest Japan, *J. Struct. Geol.*, *25*, 59–78.

Zhao, D., A. Hasegawa, and H. Kanamori (1992), Tomographic imaging of *P* and *S* wave velocity structure beneath north-eastern Japan, *J. Geophys. Res.*, *97*, 19,909–19,928, doi:10.1029/92JB00603.